Contents lists available at SciOpen

Food Science and Human Wellness

journal homepage: https://www.sciopen.com/journal/2097-0765

China Food Publishing Co.

Decoding food odor-evoked EEG signals: odor recognition and brain region analysis using Mixed Feature Attention Network (MFANet)

Yuchen Guo[a,b], Yuchao Yang[a,b], Yan Shi[a,b], Yuxiang Ying[a,b], Hong Men[a,b,*]

[a] School of Automation Engineering, Northeast Electric Power University, Jilin 132012, China
[b] Institute of Aavanced Sensor Technology, Northeast Electric Power University, Jilin 132012, China

ARTICLE INFO

Article history:
Received 13 September 2024
Received in revised form 6 November 2024
Accepted 16 December 2024

Keywords:
Food identification
Food odor
Olfactory electroencephalographic (EEG)
EEG source localization
Attention mechanism

ABSTRACT

Olfactory cues play a crucial role in food selection, with undesirable odors often being perceived as indicative of spoiled or inferior food. However, odor perception is highly subjective and prone to low reproducibility. Electroencephalographic (EEG) signals induced by odors contain rich information that can be leveraged to decode food odors. In this study, we employed EEG and source localization signals triggered by 8 different food odors as input data and proposed a Mixed Feature Attention Network (MFANet) to differentiate between food odors. Firstly, we established an experimental paradigm for olfactory EEG data collection and source localization signal processing. Secondly, we introduced a mixed feature data mining strategy, which effectively integrates both global and local features of the data. Experimental results demonstrated that MFANet achieved an average accuracy of 97.35% in distinguishing between the 8 food odors. Moreover, using standardized low resolution brain electromagnetic tomography (sLORETA) source localization, we identified significant differences in brain regions activated by different food odors, particularly in the right temporal lobe, where activation differences between pleasant and unpleasant odors were statistically significant ($t > 5$, $P < 0.001$). In conclusion, MFANet effectively mined the information contained in olfactory EEG data and successfully differentiated between the eight food odors. It also captured subtle differences in brain activation patterns induced by food odors. These findings suggest that MFANet holds potential for applications in the diagnosis and treatment of olfactory dysfunction.

1. Introduction

Anosmia, as a disease that affects an individual's ability to recognize and perceive odors, has shown a significant global prevalence trend[1]. Statistics show that anosmia not only reduces quality of life and severely affects people's perception of food flavors but may also lead to changes in eating habits and social interactions[2]. Current diagnostic methods mainly rely on subjective odor recognition tests, which are time-consuming and yield results easily influenced by test conditions and personal state. Moreover, treatment strategies like olfactory training have certain effects but generally lack targeted and individualized interventions. These challenges highlight the need for more objective and scientific methods of olfactory function assessment, especially in the field of food sensory evaluation.

In the activity of food sensory evaluation, which involves the synergistic effect of various complex physiological reactions, food odor plays a crucial role because olfaction not only affects our direct perception of food but also profoundly influences our appetite, emotions, and even memory. Olfaction, as one of the most fundamental human sensory systems, is crucial for distinguishing the safety, freshness, and quality of food. For example, odors can trigger specific emotions and memories[3], thereby guiding our food choices even in the absence of obvious visual or taste cues[4]. Therefore, enhancing the understanding and evaluation of olfactory function not

* Corresponding author at: School of Automation Engineering, Northeast Electric Power University, Jilin 132012, China
E-mail address: menhong@neepu.edu.cn (H. Men)
Peer review under responsibility of Beijing Academy of Food Sciences.

SciOpen Publishing services by Tsinghua University Press

http://doi.org/10.26599/FSHW.2025.9250482.

only helps improve the quality of life for patients with anosmia but also promotes more accurate food quality control and new product development in the food industry.

Current olfactory sensory analysis largely relies on human senses and machine perception[5]; however, both have many limitations. In human sensory evaluation, trained sensory panels usually perform quantitative descriptive analysis and preference analysis of food based on human perception[6-7]. However, since text or language descriptions are used as the basis for evaluation, discrepancies are inevitable, and ranking sensory evaluation results is often difficult due to the lack of unified evaluation criteria. In combining machine perception technology to assist in food quality control and detection[8-9], it is highly challenging to meet the production needs of different types of new products due to limitations in the number and types of sensors. Moreover, machine perception obtains material characteristics and cannot acquire psychological information, such as consumer preferences, because they lack the emotions inherent in humans. Therefore, a method that combines human perception and quantitative measurement to comprehensively evaluate the sensory characteristics of food is highly necessary.

Electroencephalographic (EEG) can effectively combine the olfactory information of substances with human sensory perception[10]. It is a non-invasive brain response research method that records brain activity using electrophysiological indicators to capture changes in brain waves, representing the overall result of neuronal electrophysiological activity in the cerebral cortex or scalp[11]. Therefore, olfactory EEG can qualitatively and quantitatively analyze the objective sensations of sensory evaluators and has strong application potential in food sensory evaluation. Consequently, functional near-infrared spectroscopy (fNIRS)[12], functional magnetic resonance imaging (fMRI)[13], and EEG source localization[14] derived from this are also often used in studies of brain region responses.

Currently, researchers in the EEG field are more inclined to apply machine learning for EEG analysis[15] because it offers better interpretability. Crouzet et al.[16] demonstrated that taste EEG induced by salty, sweet, sour, and bitter can be decoded through time-resolved multivariate pattern analysis. They used a linear classifier based on L2-regularized logistic regression to distinguish different tastes. Hashida et al.[17] used adaptive Gabor transform to extract features from taste EEG, revealing significant differences between sweet, salty, and water in EEG signal representations. However, in traditional machine learning methods, it is difficult to flexibly handle classification tasks. Even if the optimal classification features are obtained through continuous attempts and performance is partially improved, human-designed features may overlook important information in the original EEG and lack generalizability.

Deep learning models represented by Convolutional Neural Networks (CNN) have end-to-end structures, avoiding complex feature engineering. In recent years, deep learning has been widely applied in various fields and has shown significant advantages[18]. It has also demonstrated significant advantages in the field of brain science. In EEG analysis, Khare et al.[19] converted the filtered EEG signals into images through the time-frequency domain, using several different CNNs to automatically extract important features and complete emotion classification. Bang et al.[20] proposed a 3-D-CNN framework that learns important neurophysiological features by mining the spatial spectral features of motor imagery EEG. Although the above CNN models have generally achieved good results in various EEG analysis tasks, many deep learning methods are more or less disturbed by redundant information in EEG. Therefore, channel attention mechanisms have received increasing attention[21]; they enable models to focus on important features while ignoring redundant information, improving the model's classification performance[22]. Representative examples include Squeeze-and-Excitation Networks[23] and Efficient Channel Attention. It can be seen that introducing attention mechanisms in deep learning models can effectively avoid the interference of redundant information in olfactory EEG data mining. However, although many advanced models with attention mechanisms can effectively recognize raw EEG data, their structural limitation lies in the difficulty of effectively integrating global and local information due to the introduction of a single attention mechanism.

Therefore, this study proposes a mixed feature attention network based on the combination of olfactory EEG signals and source localization signals for the recognition of different kinds of food odors. By analyzing EEG responses of subjects under specific odor stimulation, we can evaluate the functional state of their olfactory pathways. Using source localization technology to accurately map complex EEG signals to specific brain regions enhances the local information of the data while discussing and analyzing brain region changes under different food odor stimuli. Subsequently, Mixed Feature Attention Network (MFANet) was constructed, fully utilizing the global characteristics of EEG signals and the local characteristics of source localization signals. By mining and integrating the global and local features of the data to obtain features that fuse global and local information for odor recognition, excellent classification performance was ultimately achieved. Furthermore, our future research will focus on expanding the types and complexity of odor stimuli, expecting to verify the effectiveness and applicability of MFANet in populations with olfactory impairment and provide patients with more personalized diagnosis and treatment recommendations. This will not only improve the diagnosis and treatment effect for patients with anosmia but also provide new scientific tools for food sensory evaluation, thereby optimizing quality control processes in the food industry.

2. Experiments and methods

2.1 Subjects and materials

This study invited 15 healthy participants aged between 21 and 25 years, including 11 males and 4 females. All participants were right-handed, non-smokers, and had no psychiatric history. The selection criteria for participants were as follows:

Age range: participants aged between 21 and 25 years were selected primarily to ensure the maturity and stability of brain development. This age range is commonly representative in neurophysiological experiments, avoiding potential influences on EEG signals caused by physiological differences in individuals who are either too young or too old.

Health status: all participants were right-handed, non-smokers, and had no psychiatric history. Right-handed individuals are typically regarded as the standard group to minimize potential interference from hemispheric functional differences. Furthermore, the criteria excluding smokers and individuals with psychiatric histories helped eliminate potential confounding factors that could affect EEG activity.

Olfactory function screening: prior to the experiment, all participants underwent 2 olfactory ability tests to ensure they could reliably distinguish the 8 odors used in the study. These tests included: 1) odor type recognition test: participants were required to identify the category of each odor when provided with the odor names; 2) odor discrimination test: participants had to determine whether two consecutively presented odors were the same or different. Participants achieving a correct response rate of ≥ 75% in both tests were considered to have normal olfactory function and met the experimental requirements.

Sample size justification: the study selected 15 participants, considering several factors. 1) Statistical power: in EEG and olfactory experiments, a relatively small sample size can still provide sufficient statistical power. For instance, Xing et al.[24] successfully explored the relationship between olfaction and EEG activity using just 8 participants in their study of odor-evoked EEG. 2) Experimental design and data characteristics: this study primarily focused on the relationship between EEG signals and olfactory stimuli, and given the substantial inter-individual variation in EEG responses, a large sample size was not necessary. During preliminary testing, we found that 15 participants were sufficient to provide stable results. Similar studies corroborate this sample size choice; for example, Hou et al.[25] used 11 participants in their olfactory EEG experiment and successfully completed the classification task. Ezzatdoost et al.[26] conducted EEG measurements of olfactory stimuli with just 5 participants. 3) Feasibility: considering the time, resources, and ethical requirements of the experiment, 15 participants were sufficient to ensure the quality of the experiment while fulfilling ethical approval requirements.

Before the experiment commenced, all volunteers signed an informed consent form and were provided with a detailed explanation of the experimental procedures. The study protocol was approved by the Northeast Electric Power University Scientific Research Ethics and Science and Technology Safety Committee and adhered to the revised Declaration of Helsinki.

In this study, we selected 8 food odors to evoke the olfactory EEG responses of participants: peppermint syrup, rose syrup, orange juice, strawberry juice, garlic sauce, shrimp paste, pickled bamboo shoots, and durian paste. Detailed information about the experimental samples is provided in Table 1. Prior to the experiment, a pre-test was conducted to establish the appropriate range for sample mass, volume, and placement time, ensuring that the odor intensity of each sample remained within a reasonable range. The specific preparation methods are as follows: 50 mL each of peppermint syrup, rose syrup, orange juice, and strawberry juice, and 25 g each of garlic sauce, shrimp paste, pickled bamboo shoots, and durian paste were prepared. The 8 materials were then placed in 250 mL sampling bottles and allowed to stand for 10 min to ensure complete odor evaporation.

Table 1
Experimental materials for food odor to induce olfactory EEG.

Label	Name	Composition	Origin
1	Shrimp paste	Fresh shrimp, edible salt	Qingdao, China
2	Sour bamboo shoot	Fresh bamboo shoots, drinking water, edible salt	Baise, China
3	Durian puree	Durian pulp	Raub, Malaysia
4	Garlic	Garlic	Linyi, China
5	Orange juice	Fructose syrup, orange juice concentrate, drinking water, food flavor	Shangqiu, China
6	Strawberry juice	Fructose syrup, strawberry juice concentrate, drinking water, food flavor	Shangqiu, China
7	Mint syrup	White sugar, food flavor, citric acid, lemon yellow, sodium carboxymethyl cellulose, drinking water	Shangqiu, China
8	Rose syrup	White sugar, food flavor, citric acid, lemon yellow, carmine, sodium carboxymethyl cellulose, drinking water	Shangqiu, China

2.2 *Instruments*

Olfactory stimulation device: to enhance experimental efficiency and ensure the reproducibility and accuracy of the results, the study designed an olfactory stimulation device. This device is characterized by low noise and high stability, capable of precisely controlling the duration and interval of stimuli. It consists of the following components: 1) air generator; 2) WS-30A gas-sensitive component test system (Zhengzhou Weisheng Electronic Technology Co., Ltd., China); 3) odor control unit; 4) odor diffuser; 5) data acquisition unit. The structure of the device is illustrated in Fig. 1. The air generator is designed to operate with minimal noise and allows easy adjustment of airflow. The activated carbon and drying tube at the air intake remove moisture from the air and adsorb nitrogen oxides, trace hydrocarbons, and esters. The WS-30A system includes a gas distribution box, a charcoal filter, a mixing fan, and a heating block. External gases are filtered through the charcoal filter before entering the gas distribution box, where the gas is evenly distributed by the mixing fan. The odor control unit consists of a gas flow controller, touch screen controller, power supply, solenoid valve, and pressure sensor. The gas flow controller comprises a flow sensor, D/A converter, flow control valve, actuator, receiver, and CPU, along with monitoring software to detect the transmission status between control units and the operation of the valves. The touch screen controller allows for the setting of stimulus duration and intervals *via* touch input. The odor diffuser delivers the gas from the sample bottles to the

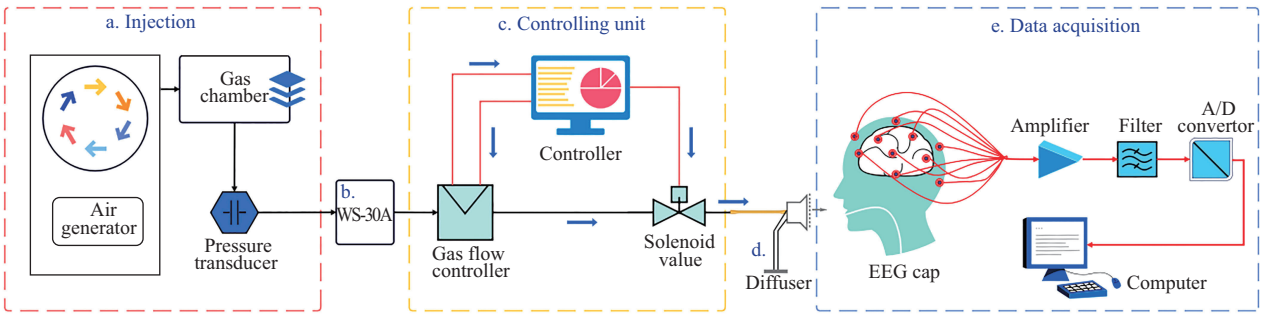

Fig. 1 Schematic diagram of the olfactory evoked instrument.

participant's nostrils, with its lower end fixed on a white acrylic base. The gas passage material is made of polytetrafluoroethylene (PTFE), which is odorless and resistant to adsorbing the sample odor. Finally, the raw EEG signals are collected by the data acquisition unit.

To further validate the applicability of the self-developed device, this study undertook several essential steps. 1) Performance testing: low noise characteristics: the noise levels of the device were measured under various operational conditions. The results demonstrated that the device operates with minimal noise, fulfilling the requirements for EEG signal acquisition without causing interference with the recorded data. During extended periods of continuous operation, the device maintained stable airflow and stimulus control, with the duration and interval of odor stimulation remaining within acceptable error margins, thereby ensuring the reproducibility and accuracy of the experiment. 2) Preliminary experiments: prior to the formal experiment, multiple preliminary trials were conducted to assess the device's performance in actual operational conditions. The EEG signals collected during these trials were clear, with no significant noise interference, thereby meeting the requirements for subsequent data analysis. 3) Comfort and safety: participant feedback during the experiment was positive, with the design of the device ensuring that they felt comfortable while receiving odor stimuli, with no adverse reactions observed.

Olfactory EEG acquisition system. Data were collected using the NCEP-P EEG acquisition system (NCC Electronics Co., Ltd., Shanghai, China) at a sampling rate of 256 Hz. According to the international 10–20 system, 21 channels (Fz, Cz, Pz, T3, T4, C3, C4, Fp1, Fp2, F7, F8, T5, T6, O1, O2, F3, F4, P3, P4, A1, A2) were placed on an EEG cap (Greentek Pty. Ltd., Wuhan, China).

2.3 Experimental procedure

The experimental paradigm in this study was designed based on relevant literature in the field of olfactory EEG research and the practical needs of the experiment[10], aiming to effectively capture high-quality odor-evoked EEG signals. The experiment ensured that participants had not eaten for 2 h, had refrained from alcohol consumption for 8 h, and were not wearing any electronic devices. Prior to the experiment, the laboratory was ventilated by opening windows and operating exhaust fans, while the temperature was controlled at (21 ± 2) ℃ through central air conditioning, ensuring no strong electromagnetic interference in the experimental environment. Participants were informed about the names of the odors they would be exposed to during the experiment. Throughout the procedure, the participants' chins were naturally placed on an adjustable chin rest. The gas diffusion end of the olfactory EEG stimulation device was positioned 2–3 cm in front of the participant's nose, while they kept their eyes closed and breathed steadily. For each participant, the experimental process, as shown in Fig. 2, included 8 randomly arranged odor stimuli, with each odor stimulus being repeated 20 times in parallel to minimize the impact of single-trial errors on the overall results. Resting EEG data from the 10 s prior to each odor stimulus served as baseline data. Each parallel experiment for a given odor lasted 10 s, with a 5 s interval between each repetition. At the start of each stimulus, the operator marked the event in the EEG data by pressing a button. It is worth noting that the time error of the event marker (typically within a few hundred milliseconds) was relatively small compared to the entire stimulus duration (10 s), and thus its effect on subsequent analysis was negligible. There was a 5 min interval between each odor experiment to allow participants to rest. During this rest period, the door and fan were opened, the sampling bottles were removed, and the residual odors in the olfactory EEG stimulation device were cleared by operating the air generator. After the rest period, the procedure was repeated in the sequence of odors until all 8 odors had been tested.

2.4 Data preprocessing

This study utilized MATLAB (R2022B) and its built-in toolbox, EEGLAB (version 2022), to preprocess the raw EEG data obtained from olfactory stimuli in order to derive the "clean" data for subsequent analysis. The specific processing steps are as follows:

Data acquisition and sample construction: 1) Participants and number of trials: EEG data were collected from 15 participants under 8 different food odor stimuli, with each odor stimulus being presented 20 times in parallel. 2) Signal extraction time window: for each parallel trial, EEG signals from 1 to 9 s of the stimulus were retained to effectively capture stable brain activity, avoiding interference from the transient effects at the onset and offset of the stimuli. 3) Sample division: the length of each EEG sample was set to 1 s, yielding 8 independent samples for each parallel trial. The samples were labeled based on the odor type, with labels assigned sequentially from 0 to 7. 4) Total number of samples: in total, 19 200 olfactory EEG samples were obtained (15 participants × 8 odors × 20 trials × 8 samples per trial).

Signal filtering: 1) FIR filter: a finite impulse response (FIR) filter, implemented in MATLAB-EEGLAB, was applied to process the EEG signals. This type of filter is widely utilized in EEG signal processing for its effectiveness in removing unwanted noise while preserving the integrity of the underlying neural signals[27]. 2) Low-pass filtering: a low-pass filter with a cutoff frequency of 47 Hz was initially applied to remove high-frequency noise. The cutoff frequency for the signal was set at 52.875 Hz, allowing for the retention of crucial frequency bands associated with cognitive and perceptual processes[10]. 3) Notch filtering: a 50 Hz notch filter was employed to eliminate power line noise, thereby removing interference from the mains frequency and ensuring the signal's fidelity[28].

Sampling rate adjustment: the filtered EEG data were reduced from a sampling rate of 256 to 128 Hz to decrease the data volume and enhance computational efficiency, while preserving the essential features of the signal.

Artifact handling: 1) Visual inspection and removal: EEG signals were visually inspected to identify and exclude trials with obvious artifacts, such as those caused by eye blinks, muscle activity, or motion artifacts. Only high-quality signals were retained for further analysis[29]. 2) Independent component analysis (ICA): ICA was employed to separate and remove components associated with ocular and electromyographic artifacts, thereby enhancing the purity of the EEG signals[30].

Baseline correction: prior to each odor-induced EEG experiment, the 10 s resting-state EEG data preceding the odor stimulus were used as baseline for the correction of the EEG signals. This step helps eliminate the effects of electrode shifts and slow-wave drift, ensuring that the subsequent voltage changes reflect true neural responses, free from the influence of non-olfactory sensory stimuli[31].

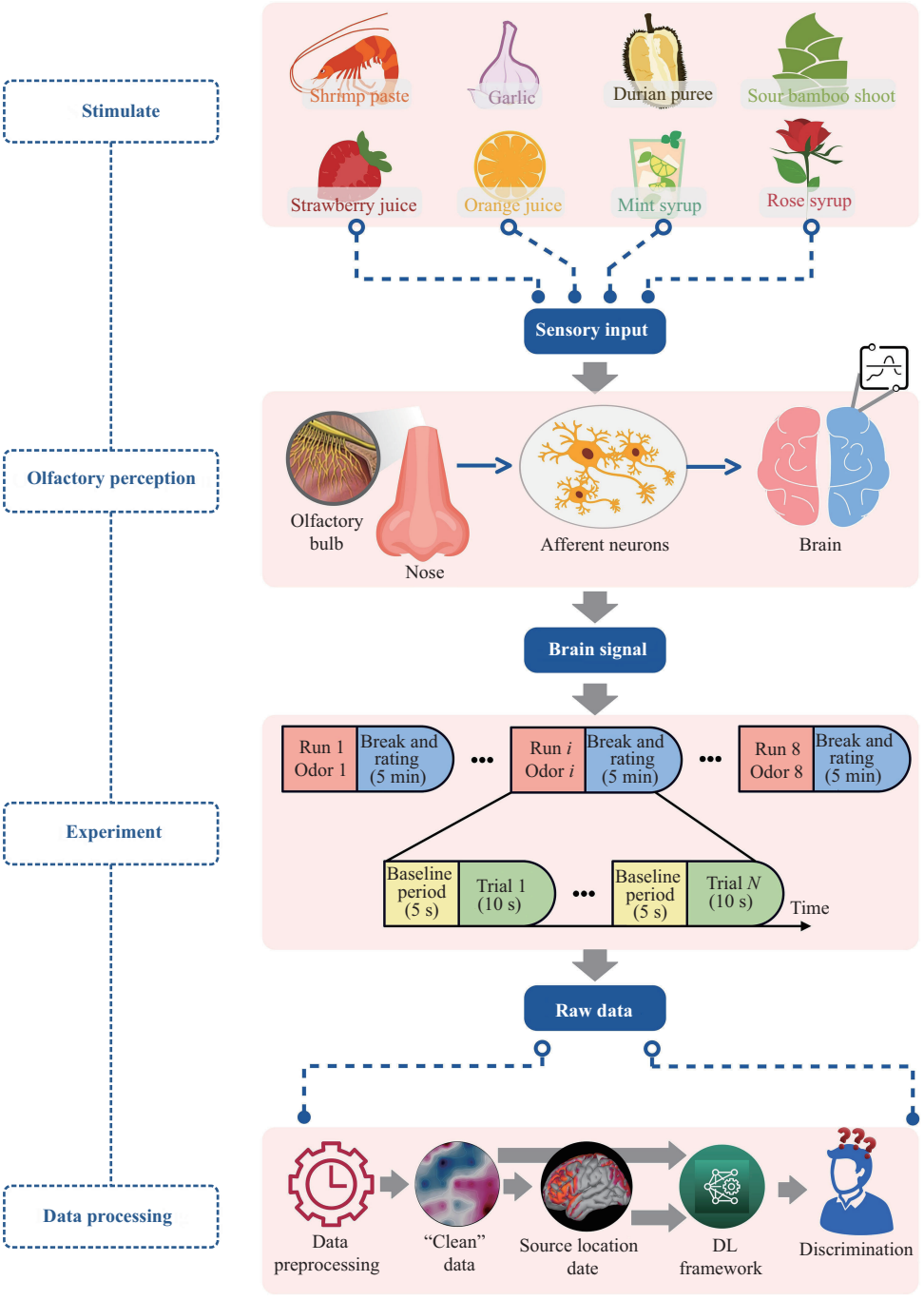

Fig. 2 Experimental procedure flowchart.

2.5 *EEG source localization*

EEG source localization is a non-invasive neuroimaging technique used to determine the spatial location of electrical activity within the brain[32]. In this study, we used Matlab-Brainstorm to perform source localization analysis on the olfactory EEG generated by different subjects under different odor stimuli. The following are the steps of the source localization process:

1) Data acquisition: electrical activity data were collected from multiple scalp locations using a multi-channel EEG device. These data $V(t)$ reflect the scalp projections of internal brain electrical activity at specific time points.

2) To map the measured scalp potentials V to brain sources J, a head model containing the conductivities of the skull, cortex, and brain tissue needs to be established. This model can be expressed as the lead field matrix H, which describes the current transfer paths from brain sources to scalp electrodes. The calculation formula (1):

$$V = HJ + E \quad (1)$$

Where, V is the potential vector measured by scalp electrodes; H is the lead field matrix; J is the current source vector generated by brain electrical activity, and E is the measurement noise.

3) Inverse problem solving: the goal of the inverse problem is to estimate the brain source J from the given scalp potentials V. This typically involves regularization techniques to solve the

underdetermined problem. A commonly used method is standardized low resolution brain electromagnetic tomography (sLORETA), which takes into account the spatial smoothness of the sources[33], and can be expressed as formula (2):

$$\hat{J} = \sigma^{-2}CH^{T}(HCH^{T} + \sigma^{2}I)^{-1}V \quad (2)$$

Where C is the prior covariance matrix of the source signals, σ^2 is the noise variance, and I is the identity matrix.

4) Result analysis: once the source estimate $\hat{J}$ is obtained, the next step is to visualize these activities using imaging techniques. By mapping the source activity onto a three-dimensional brain model, one can intuitively view and analyze the activities of different brain regions under specific tasks or states.

5) Data export: export the source-localized brain regions into MATLAB. The final data input into subsequent models is expanded from the preprocessed 128 × 21 to 128 × 148. The 148 represents the classification by Destrieux et al.[34], who categorized each vertex of brain regions into sulci or gyri and then subdivided them into 74 labels per hemisphere, totaling 148 labels.

2.6 Mix feature attention network

1) Overall network description: olfactory EEG induced by odor stimulation is usually composed of EEG signals generated by neuronal networks in each brain region through potential changes from a local perspective, and the connections and cooperation between different brain regions from a global perspective. The activities of local brain regions influence and are influenced by other regions through the global integration of neural networks, forming complex EEG waveforms. Extracting local and global features of EEG signals through a single network has significant limitations and cannot comprehensively characterize the properties of EEG signals. Therefore, MFANet is proposed to fully exploit and combine the global and local features of EEG signals to better accomplish complex classification tasks. The structure of MFANet is shown in Fig. 3 and consists of 3 parts: shallow feature extraction, multi-scale feature fusion, and deep feature extraction. The specific process is as follows. First, MobileNet V2[35] and GCN[36] were used to extract the local unimodal features m and global unimodal features b of EEG signals, respectively; secondly, a multi-view mixing of features was performed to obtain features that combine global and local information; third, by overlaying the local information and mixed features again, the mapping of local information in the global space is obtained; finally, the mapping information was concatenated with the global vector, and through a self-attention mechanism, a feature vector that blends global and local information is obtained to recognize EEG signals generated under different food odor stimulations.

2) Shallow feature mining (SFM) consists of 2 networks designed for extracting global and local features. Because the source localization signals are more complex and contain more features, MobileNet V2 with depthwise separable convolutions and inverted residual structures is more suitable for extracting the local features m of the source localization signals. In contrast, using a GCN to treat the raw EEG signals as a graph structure and iteratively aggregate information from nodes and their neighboring nodes enables each node to integrate features from distant nodes, making it more suitable for capturing the global features b in the entire data structure. In this process, the input multimodal samples of the source localization signals and raw EEG signals are respectively reshaped into (1, 148, 128) and (1, 21, 128). Then, adjust the convolution kernel size, stride, padding size, output channels, pooling kernel size, and pooling stride so that the extracted multimodal initial features have the same size. Finally, reshape the unimodal features output by MobileNet V2 and GCN into (1, 16, 32) to obtain the shallow features of the source localization signals and the initial EEG signals.

3) Multi-Scale Feature Mixing (MFM) mainly consists of a Mixed Feature Attention Module and a self-attention module, which are connected alternately. The output Z_1 of the first Mixed Feature Attention Module is the input to the first self-attention module. Then, the output S_1 of the first self-attention module, along with the global feature b, serves as the input to the second Mixed Feature Attention Module. Finally, the output Z_2 of the second Mixed Feature Attention Module is fed into the second self-attention module to obtain the final output S_2.

The structure of the Mixed Feature Attention Module is shown in Fig. 4a, mainly including Embedding, Layer Normalization (LN),

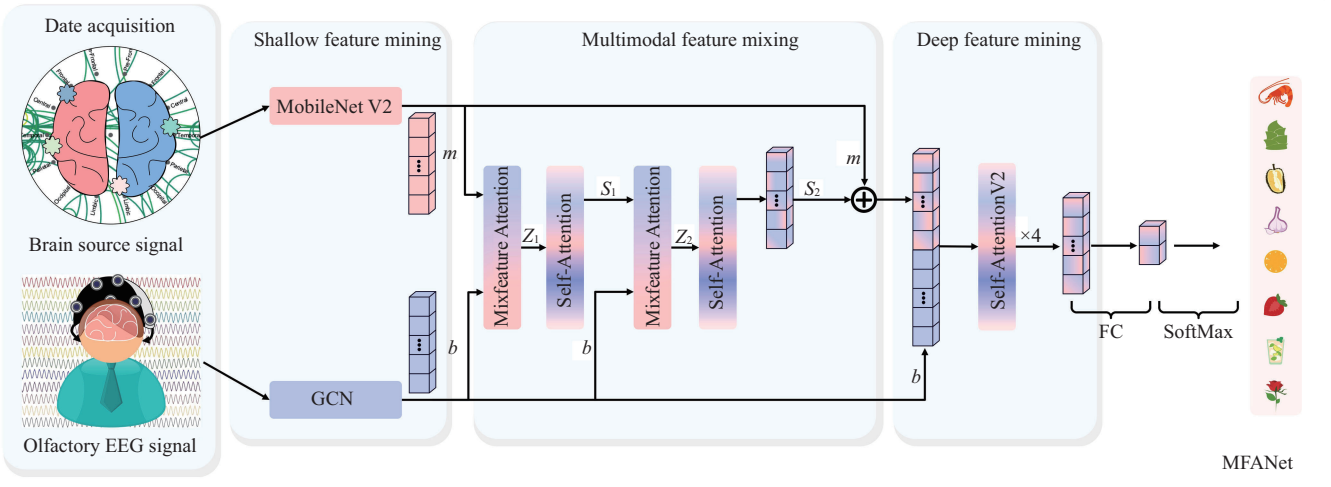

Fig. 3 Overview of the proposed MFANet.

Linear Layers, Multi-head Attention (MHA), and Multi-layer Perceptron (MLP). First, m and b of size 1 × 16 × 32 were reconstructed into 2D sequences through 2D convolution. The kernel size and stride of the 2D convolution are 1 × 2. The reconstructed sequence contains 256 tokens to ensure that each feature information was efficiently reconstructed. The output channels of the 2D convolution are set to 512 to ensure effective information retention. Then, classification tokens are added before the reconstructed sequence for classification. Therefore, after Embedding, unimodal features in the form of 257 × 512 data are obtained. Next, LN normalization is applied to the unimodal features to ensure the stability of feature distribution. In LN, the normalized features are multiplied by optimizable matrices to obtain 3 inputs: Q, K, and V. Here, Q is the query value for finding common features that reflect subjects' olfactory preferences, K is the key feature information in olfactory EEG, and V represents all features in olfactory EEG. Third, Q, K, and V are input into MHA to mine common features while retaining underlying features. The output X of MHA was added to Embedding (m) to obtain Y. Then, Y passes through LN and MLP, where MLP consists of 2 fully connected (FC) layers with a GELU activation function inserted between them to make the model training process more robust. Finally, the output of MLP is added to Y to obtain the output Z of the Mixed Feature Attention Module. The calculation formula is shown in equations (3) and (4):

$$Y = \mathrm{MHA}\,(Q, K, V) + \mathrm{Embedding}\,(m) \tag{3}$$

$$Z = \mathrm{MLP}\,(\mathrm{LN}(Y)) + Y \tag{4}$$

Where, Q represents the query value obtained after Embedding, LN, and Linear operations on the source localization data in the Mixed Feature Attention Module; it is used to identify common features reflecting the subjects' olfactory preferences. K and V represent the key feature information (K) and all features (V) of the olfactory EEG data extracted in the cross-modal attention module, respectively, with steps including Embedding, LN, and Linear m denotes the source localization signal features output by MobileNet V2.

MHA is the key component in the cross-modal attention module that fully utilizes multimodal features. Compared to single-head attention, the multi-head attention in MHA enables the model to fully establish interactions between complex subspaces of different modalities. The computational process of MHA is shown in Fig. 4c. First, the inputs Q, K, and V are expanded from 257 × 512 to 257 × 8 × 64 along the second dimension. Then, swap the first and second dimensions of the expanded features to obtain multiple head features Q_h, K_h, and V_h, where the number of heads is 8. Next, swap the second and third dimensions of K_h. After swapping, multiply K_h by Q_h, and scale by dividing by d. Third, input the scaled values into the SoftMax layer and multiply by Q_h to obtain a multi-head feature. Finally, concatenate the first and third dimensions of the multi-head features to integrate the sub-features, multiply the integrated features by an optimizable matrix W_h, and obtain the linearized output X, whose calculation formula is shown in equation (5):

$$X = \mathrm{Concat}(\mathrm{SoftMax}\left(\frac{Q_h \times K_h^T}{d}\right) \times V)_h \times W_h \tag{5}$$

Where T represents the second and third dimensions are interchanged, $d = \sqrt{40}$, Concat represents merging the first and third dimensions of the feature matrix. Q_h, K_h and V_h are multi-head features obtained by expanding Q, K and V along the second dimension from 257 × 512 to 257 × 8 × 64, respectively, and then exchanging the first and second dimensions of the expanded features. W_h is optimizable matrice.

The self-attention module is similar to the cross-modal attention module, as shown in Fig. 4b, with the Embedding, LN, Linear, MHA, and MLP sharing the same structure. The difference is that the input to the self-attention module is a unimodal feature matrix, and only one Embedding, LN, and Linear are connected in sequence.

4) Deep Feature Mining (DFM) is composed of four sequentially connected Self-AttentionV2 modules. For DFM, the feature sequences S_2 and b are reconstructed and concatenated into a 1 × 1 024 feature sequence, which is then reshaped into a 1 × 16 × 64 feature matrix as the input to the DFM module. The Self-AttentionV2 module is similar to the self-attention module in the MFM module, with only slight differences in the Embedding module. In the Embedding module, the kernel size and stride of the 2D convolution are set to 2 × 4, and the output channels are set to 512, resulting in 128 tokens in the reconstructed sequence. A classification token is then added before the reconstructed sequence, resulting in a feature sequence of size 129 × 512. After passing through the four sequential Self-AttentionV2 modules, the 1 × 512 classification token is input into the FC layer. Finally, olfactory preference prediction is performed through the SoftMax layer.

In this study, all models were implemented using Pytorch 1.13.0 and trained on an NVIDIA GeForce RTX 4070Ti GPU. The training set

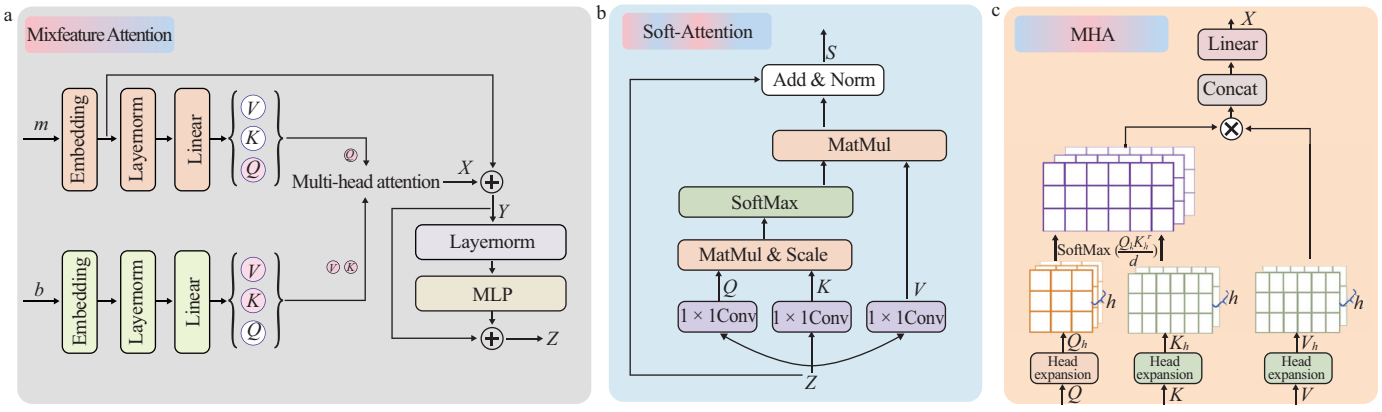

Fig. 4 (a) Architectural elements of Misfeature Attention; (b) Architectural elements of Self-Attention; (c) Architectural elements of MHA.

and test set were split in a 7:3 ratio. In the training of the classification model, the Adam optimizer was used for weight updates and parameter optimization, with 200 iterations involved in the training process. The cross-entropy loss function and L2 regularization were used to calculate the error, with the regularization parameter set to 0.001. Without loss of generality, the mean accuracy, recall, and precision of 10 iterations were calculated as the final classification results.

3. Results and discussion

3.1 Source localization analysis of brain responses to the different food odor

This section of the work is a derivative result of MFANet, utilizing the EEG source localization technique from MFANet. Employing a realistic human head model, it depicts the structural regions of the entire cortical area, providing a more intuitive observation of the brain region mapping results under different food odor stimuli.

EEG source localization was performed using sLORETA to examine whether eight different food odors are encoded in distinct regions of the cortical brain areas. As shown in Fig. 5, the primary brain regions associated with Shrimp Paste include the left superior frontal gyrus (SFG-L), left rostral middle frontal gyrus (RMFG-L), left middle temporal gyrus (MTG-L), left inferior temporal gyrus (ITG-L), left superior temporal gyrus (STG-L), right pretriangular area (PTRI-R), right superior frontal gyrus (SFG-R), right superior temporal gyrus (STG-R), right middle temporal gyrus (MTG-R), and right inferior temporal gyrus (ITG-R). The main brain regions related to Garlic include the MTG-L, ITG-L, STG-L, left lateral orbitofrontal gyrus (LOFG-L), PTRI-R, STG-R, MTG-R, and ITG-R. The key brain regions for Durian Puree are the SFG-L, RMFG-L, MTG-L, ITG-L, STG-L, left inferior parietal lobule (IPL-L), SFG-R, STG-R, MTG-R, ITG-R, and right supramarginal gyrus (SMG-R). The regions associated with Sour Bamboo Shoot include the SFG-L, RMFG-L, MTG-L, STG-L, IPL-L, PTRI-R, STG-R, MTG-R, ITG-R, and SMG-R. For strawberry juice, the primary regions are the MTG-L, ITG-L, STG-L, left prefrontal orbital area (POPER-L), left pretriangular area (PTRI-L), right lateral occipital gyrus (LOG-R), right inferior parietal lobule (IPL-R), right postcentral gyrus (PoCG-R), and right precentral gyrus (PrCG-R). The regions associated with Orange Juice include the MTG-L, ITG-L, STG-L, PTRI-L, LOG-L, right cingulate gyrus (iCG-R), right RMFG-R, orbitofrontal gyrus (LOFG), and superior frontal gyrus (SFG). The key regions related to Mint Syrup are the MTG-L, ITG-L, STG-L, PTRI-L, LOG-L, iCG-R, and SFG. Finally, for Rose Syrup, the main regions are the MTG-L, ITG-L, STG-L, POPER-L, PTRI-L, iCG-R, and LOG-R.

To further validate whether the activation differences in these brain regions are significant and to address potential issues of false positives, paired-sample *t*-tests with Bonferroni correction were conducted to compare the activation values of each brain region under different odor conditions. The results indicated that there are distinct differences in brain region activation across different food odors. Notably, compared to unpleasant odors, pleasant odors elicited minimal activation in right-sided regions such as the STG-R, MTG-R, and ITG-R, whereas unpleasant odors showed significant activation in these areas. Specifically, the results of the paired-sample *t*-test are as follows: for the STG-R region, the activation value for unpleasant odors was significantly higher than for pleasant odors ($t = 27.163$, $P < 0.001$); for the MTG-R region, the activation value for unpleasant odors was significantly higher than for pleasant odors ($t = 32.029$, $P < 0.001$); and for the ITG-R region, the activation value for unpleasant odors was significantly higher than for pleasant odors ($t = 6.014$, $P < 0.001$). After applying the Bonferroni correction, each P-value was compared to the corrected significance threshold. Given that this study involved 148 brain regions, the significance threshold was set at 0.000 338 (i.e., 0.05/148) to control for false positives due to multiple comparisons. The corrected analysis still showed that activation in the STG-R, MTG-R, and ITG-R regions was significantly higher for unpleasant odors than for pleasant odors, with this difference remaining highly significant statistically. The Bonferroni-corrected *P*-values were as follows: for the STG-R region, the corrected *P*-value < 0.000 338; for the MTG-R region, the corrected *P*-value < 0.000 338; and for the ITG-R region, the corrected *P*-value < 0.000 338.

These results further validate the significant differences between pleasant and unpleasant odors in the cortical brain regions, particularly in the right temporal lobe regions STG-R, MTG-R, and ITG-R, indicating that the response intensity in these areas is significantly higher for unpleasant odors compared to pleasant ones. The Bonferroni-corrected analysis maintained statistical significance, effectively eliminating the potential for false positives and thereby enhancing the reliability and accuracy of the study's findings.

The findings of this study underscore the complex interplay between olfaction, emotion, and memory, particularly within the context of emotional memory processing. The olfactory system, due to its direct connections with key emotional memory regions of the brain, such as the hippocampus and amygdala, is capable of triggering intense emotional responses. Similar conclusions have been drawn by previous research; for instance, Herz et al.[37] highlighted the relationship between olfactory information and emotional memory, making olfaction a powerful trigger for emotional and memory responses, particularly through the involvement of the hippocampus and prefrontal cortex. Owen[38] further emphasized that olfaction is a sensory system closely linked to emotional memory, with olfactory signals directly connected to the brain's emotional processing regions (e.g., amygdala) and memory-related areas (e.g., hippocampus), thus enabling olfaction to evoke strong emotional and memory responses. These connections are especially pronounced in the role of the hippocampus and prefrontal cortex, which play a critical role in the encoding and processing of emotional memory.

Moreover, this study places particular emphasis on the temporal and frontal lobe regions (especially the STG, MTG, and SFG), which may play crucial roles in the interaction between olfactory information and emotional memory circuits, influencing the perception of odors and emotional responses. Olfactory information is not processed in isolation; it interacts with other sensory inputs, such as vision and hearing, to shape the overall perception and emotional response to external stimuli. The parietal regions (e.g., IPL) and temporal lobe regions (e.g., STG and MTG) play key roles in this integrative process, combining olfactory information with other sensory inputs to jointly regulate perception and emotional responses. Similar research

has been conducted, Stein et al.[39] noted that during multisensory integration, the interaction between olfaction and vision or hearing influences the overall perception of stimuli and emotional responses, particularly with the involvement of parietal and temporal regions. Murray et al.[40] further suggested that the parietal cortex (e.g., IPL) and temporal cortex (e.g., STG, MTG) are pivotal in the integration of multisensory information, particularly in emotional and cognitive tasks, enabling the combination of olfactory and other sensory information to elicit more complex responses to external stimuli.

In conclusion, integrating the findings from existing literature, this study supports the significant role of brain regions such as the STG, MTG, and ITG in the processing of olfactory information, emotional responses, and multisensory integration. It further deepens the understanding of the neural mechanisms underlying the emotional and cognitive effects of olfactory stimuli in the brain, and highlights the complex role of multisensory integration in memory processing.

3.2 Ablation experiment

To evaluate the effectiveness of MFM and DFM in the overall method, we conducted two ablation experiments as shown in Table 2, highlighting the importance of MFM in mixing local and global information at the attention level and DFM in extracting features at the output feature level. First, the study discusses the importance of the MFM module, which is used to mix local and global features to obtain information from the samples that better represents EEG signals.

As shown in Table 2, if only the fusion of global and local information at the feature level is considered, the model's accuracy is 93.82%, recall is 93.78%, and precision is 92.45%, with a relatively significant standard deviation, indicating poor model stability. This may be due to the lack of representations that can capture both global and local features, leading to relatively independent extraction of deep information. The information becomes overly smooth, resulting in the omission of key local details and, ultimately, a decline in classification performance.

Next, the study explores the effectiveness of the DFM module, which aims to obtain feature vectors that blend global and local information from the perspective of feature concatenation and mining. As shown in Table 2, if only the mixing of global and local features is considered without effectively mapping the feature vectors in space, the model's classification performance shows accuracy of 92.33%, recall of 92.32%, and precision of 92.33%, with the overall model still exhibiting suboptimal classification performance. Therefore, the design of the DFM module is necessary for more effective classification tasks.

Table 2
Results of the ablation experiments on different structures in MFANet.

No.	MFM	DFM	Accuracy (%)	Recall (%)	Precision (%)
1	×	√	93.82 ± 1.32	93.78 ± 1.44	92.45 ± 0.88
2	√	×	92.33 ± 0.73	92.32 ± 1.03	92.33 ± 1.10
3	√	√	**97.35 ± 0.44**	**97.33 ± 0.68**	**97.36 ± 0.79**

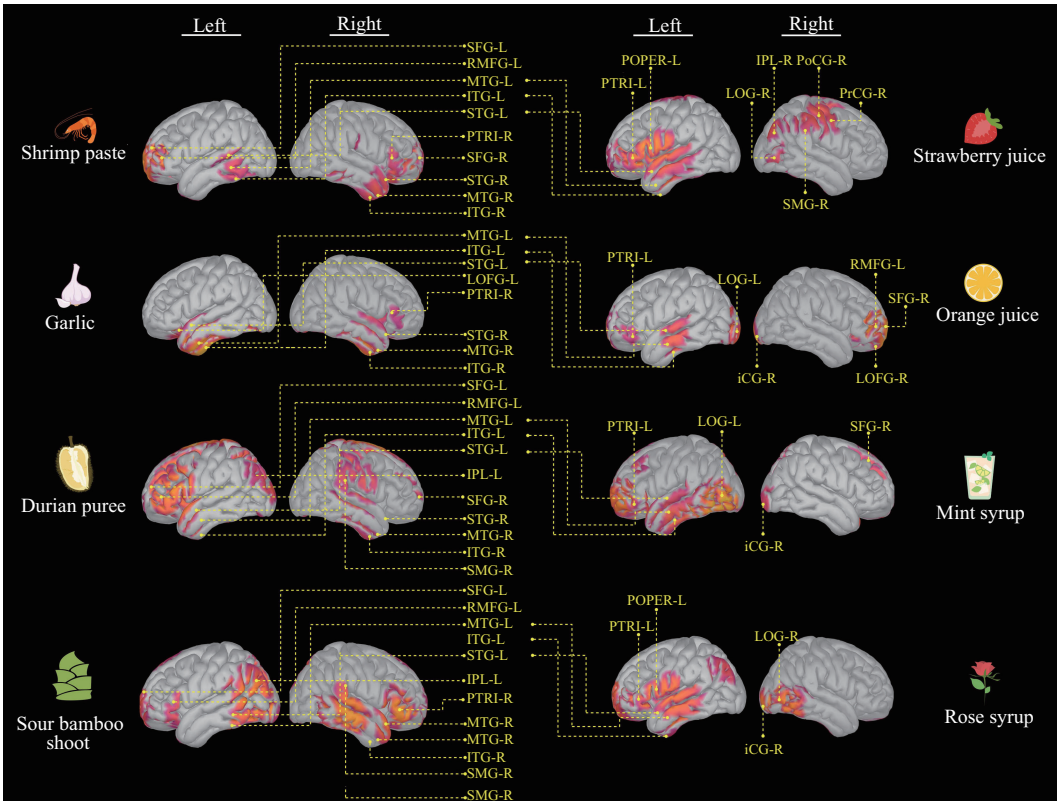

Fig. 5 Sources of neural activity related to the stimulation of different food odors in the brain.

Finally, as shown in Table 2, under the synergy of MFM and DFM, the model achieved the best classification results, with an accuracy of 97.35%, recall of 97.33%, and precision of 97.36%. In conclusion, MFANet effectively integrates local and global information and represents it in the corresponding vector space. While achieving complementarity, it also deeply integrates olfactory EEG signals with source localization signals.

3.3 Classification results

The results presented in Table 3 demonstrate that MFANet achieves the highest classification performance, with an accuracy of 97.35%, recall of 97.33%, and precision of 97.36%. In this study, we compared classic CNN architectures with the more advanced Transformer architectures, as well as architectures specifically designed for processing olfactory EEG data[21], to fully showcase the performance of our proposed model. We ensured that all models were compared under identical training conditions, with hyperparameters optimized for each model.

Among the CNN-based models, we selected three models for comparison: LeNet-5, ResNet18, and EEGNet. ResNet18, widely applied in EEG tasks, primarily utilizes residual connections to avoid the vanishing gradient problem in deep networks. EEGNet, a compact and general-purpose CNN designed for EEG signal recognition, extracts both time and spatial features of EEG signals by learning time and spatial filters. As shown in Table 3, MFANet significantly outperforms these three models. For Transformer-based models, we compared Vision-Transformer and Restormer. Vision-Transformer, with its classical architecture, requires a high model complexity for EEG signal recognition tasks, which severely impacts its classification performance. In contrast, Restormer, a lightweight transformer-based model, achieved an accuracy of 94.84%. This highlights that a hybrid structure combining convolutions and Transformers is more effective in capturing feature information. Additionally, we compared MFANet with state-of-the-art methods described in the introduction and references for processing olfactory EEG signals. The results in Table 3 indicate that MFANet outperforms these methods in classification performance. In summary, MFANet successfully integrates and mines both global and local information, effectively accomplishing the food odor classification task.

Table 3
Classification results of different classification methods.

Methods	Accuracy (%)	Recall (%)	Precision (%)
LeNet-5	92.27 ± 1.21	92.23 ± 1.21	92.26 ± 1.05
EEGNet	93.44 ± 1.21	93.55 ± 1.08	93.64 ± 1.13
ResNet18	94.18 ± 1.08	94.15 ± 1.07	94.29 ± 1.12
Vision-Transformer	94.34 ± 0.87	94.44 ± 1.17	94.13 ± 0.97
Resformer	94.84 ± 0.51	94.66 ± 0.54	94.79 ± 0.50
Xia et al.[21]	95.43 ± 1.08	95.44 ± 1.08	95.84 ± 1.02
MFANet	**97.35 ± 0.44**	**97.33 ± 0.68**	**97.36 ± 0.79**

4. Conclusion

This study proposes a hybrid feature attention network, MFANet, based on the combination of EEG and source localization signals, for distinguishing olfactory EEG signals under different food odor stimuli. The main conclusions are as follows:

1) MFANet achieves an average accuracy of 97.35% in identifying 8 types of olfactory EEG signals, significantly outperforming previous models, thereby validating the effectiveness of this method in food odor recognition.

2) Through the hybrid feature data mining strategy, the global characteristics of EEG signals and the local features of source localization signals are successfully integrated, enhancing the model's ability to differentiate odors.

3) Using the sLORETA source localization technique, significant activation differences between pleasant and unpleasant odors in regions such as STG-R, MTG-R, and ITG-R were found ($t > 5$, $P < 0.001$), revealing distinct neural response patterns when the brain perceives different odors.

This study investigates food odors by analyzing EEG signals, focusing on the overall odor stimulus. Although certain results have been achieved, there are still limitations, especially in terms of not considering the effects of specific aromatic compounds on brain regions. Future research could further explore the composition of odors and delve into the effects of specific aromatic compounds on brain regions, which will provide more precise physiological evidence for olfactory perception. The significance of this study lies in providing an innovative technical approach for the objective analysis of food odors, laying the theoretical foundation for future interdisciplinary research combining olfactory perception and brain science. In addition, this method holds important application potential in the diagnosis and treatment of olfactory dysfunction, offering support for clinical practices in related fields.

Declarations of competing interest

The authors declare that they have no known competing financial interests or personal relationships that could have appeared to influence the work reported in this paper.

Acknowledgements

This work was supported in part by the National Natural Science Foundation of China (32471150) and the Science and Technology Development Plan of Jilin Province (YDZJ202101ZYTS135).

References

[1] C. Marin, I. Alobid, M. Fuentes, et al., Olfactory dysfunction in mental illness, Curr. Allergy Asthma Rep. 23(3) (2023) 153-164. https://doi.org/10.1007/s11882-023-01068-z.

[2] D. Rofey, V. Kisler-van Reede, J. Landsbaugh, Perceptions and metaperceptions of same-sex social interactions in college women with disordered eating patterns, Body Image 4(1) (2007) 61-68. https://doi.org/10.1016/j.bodyim.2006.11.001.

[3] S. Chu, J.J. Downes, Proust nose best: odors are better cues of autobiographical memory, Mem. Cognit. 30(4) (2002) 511-518. https://doi.org/10.3758/bf03194952.

[4] M.L. Demattè, D. Sanabria, C. Spence, Olfactory discrimination: when vision matters? Chem. Senses 34(2) (2009) 103-109. https://doi.org/10.1093/chemse/bjn055.

[5] E. Scholten, Composite foods: from structure to sensory perception, Food Funct. 8 (2017) 481-497. https://doi.org/10.1039/C6FO01099G.

[6] R. Puri, K. Khamrui, Y. Khetra, et al., Quantitative descriptive analysis and principal component analysis for sensory characterization of Indian milk product cham-cham, J. Food Sci. Technol. 53(2) (2016) 1238-1246. https://doi.org/10.1007/s13197-015-2089-4.

[7] H. Yuan, X. Chen, Y. Shao, et al., Quality evaluation of green and dark tea grade using electronic nose and multivariate statistical analysis, J. Food Sci. 84(12) (2019) 3411-3417. https://doi.org/10.1111/1750-3841.14917.

[8] H. Men, M. Liu, Y. Shi, et al., Interleaved attention convolutional compression network: an effective data mining method for the fusion system of gas sensor and hyperspectral, Sensor. Actuat. B-Chem. 355 (2022) 131113. https://doi.org/10.1016/j.snb.2021.131113.

[9] W. Luo, J. Zhang, H. Huang, et al., Prediction of fat content in salmon fillets based on hyperspectral imaging and residual attention convolution neural network, LWT-Food Sci. Technol. 184 (2023) 115018. https://doi.org/10.1016/j.lwt.2023.115018.

[10] X. Xia, Y. Guo, Y. Wang, et al., Advancing cross-subject olfactory EEG recognition: a novel framework for collaborative multimodal learning between human-machine, Expert Syst. Appl. 250 (2024) 123972. https://doi.org/10.1016/j.eswa.2024.123972.

[11] M.E. Peltola, M. Leitinger, J.J. Halford, et al., Routine and sleep EEG: minimum recording standards of the International Federation of Clinical Neurophysiology and the International League Against Epilepsy, Epilepsia 64(3) (2023) 602-618. https://doi.org/10.1111/epi.17448.

[12] R. Li, C. Zhao, C. Wang, et al., Enhancing fNIRS analysis using EEG rhythmic signatures: an EEG-informed fNIRS analysis study, IEEE Trans. Biomed. Eng. 67(10) (2020) 2789-2797. https://doi.org/10.1109/TBME.2020.2971679.

[13] M.R. Bennett, S. Hatton, D.F. Hermens, et al., Behavior, neuropsychology and fMRI, Prog. Neurobiol. 145-146 (2016) 1-25. https://doi.org/10.1016/j.pneurobio.2016.07.001.

[14] M.A. Jatoi, N. Kamel, A.S. Malik, et al., EEG-based brain source localization using visual stimuli, Int. J. Imaging Syst. Technol. 26(1) (2016) 55-64. https://doi.org/10.1002/ima.22157.

[15] Y. Guo, X. Xia, Y. Shi, et al., Olfactory EEG induced by odor: used for food identification and pleasure analysis, Food Chem. 455 (2024) 139816. https://doi.org/10.1016/j.foodchem.2024.139816.

[16] S.M. Crouzet, N.A. Busch, K. Ohla, Taste quality decoding parallels taste sensations, Curr. Biol. 25(7) (2015) 890-896. https://doi.org/10.1016/j.cub.2015.01.057.

[17] J.C. Hashida, A.C. de Sousa Silva, S. Souto, et al., EEG pattern discrimination between salty and sweet taste using adaptive Gabor transform, Neurocomputing 68 (2005) 251-257. https://doi.org/10.1016/j.neucom.2005.04.004.

[18] Z. Wang, Y. Yu, J. Liu, et al., Peanut origin traceability: a hybrid neural network combining an electronic nose system and a hyperspectral system, Food Chem. 447 (2024) 138915. https://doi.org/10.1016/j.foodchem.2024.138915.

[19] S.K. Khare, V. Bajaj, Time-frequency representation and convolutional neural network-based emotion recognition, IEEE Trans. Neural Netw. Learn. Syst. 32(7) (2021) 2901-2909. https://doi.org/10.1109/TNNLS.2020.3008938.

[20] J.S. Bang, M. H. Lee, S. Fazli, et al., Spatio-spectral feature representation for motor imagery classification using convolutional neural networks, IEEE Trans. Neural Netw. Learn. Syst. 33(7) (2022) 3038-3049. https://doi.org/10.1109/TNNLS.2020.3048385.

[21] X. Xia, Y. Shi, P. Li, et al., FBANet: an effective data mining method for food olfactory EEG recognition, IEEE Trans. Neural Netw. Learn. Syst. 35(10) (2024) 13550-13560. https://doi.org/10.1109/TNNLS.2023.3269949.

[22] H. Wang, C. Lu, Q. Zhang, et al., A novel sleep staging network based on multi-scale dual attention, Biomed. Signal Process. Control 74 (2022) 103486. https://doi.org/10.1016/j.bspc.2022.103486.

[23] J. Hu, L. Shen, G. Sun, Squeeze-and-excitation networks, Proc. IEEE Conf. Comput. Vis. Pattern Recognit. 2018 (2018) 7132-7141. https://doi.org/10.1109/CVPR.2018.00745.

[24] M. Xing, S. Hu, B. Wei, et al., Spatial-frequency-temporal convolutional recurrent network for olfactory-enhanced EEG emotion recognition, J. Neurosci. Methods 376 (2022) 109624. https://doi.org/10.1016/j.jneumeth.2022.109624.

[25] H. Hou, X. Zhang, Q. Meng, Olfactory EEG signal classification using a trapezoid difference-based electrode sequence hashing approach, Int. J. Neural Syst. 30(3) (2020) 2050011. https://doi.org/10.1142/S0129065720500112.

[26] K. Ezzatdoost, H. Hojjati, H. Aghajan, Decoding olfactory stimuli in EEG data using nonlinear features: a pilot study, J. Neurosci. Methods 341 (2020) 108780. https://doi.org/10.1016/j.jneumeth.2020.108780.

[27] A. Widmann, E. Schröger, Filter effects and filter artifacts in the analysis of electrophysiological data, Front. Psychol. 3 (2012) 233. https://doi.org/10.3389/fpsyg.2012.00233.

[28] A. Notbohm, J. Kurths, C.S. Herrmann, Modification of brain oscillations *via* rhythmic light stimulation provides evidence for entrainment but not for superposition of event-related responses, Front. Hum. Neurosci. 10 (2016) 10. https://doi.org/10.3389/fnhum.2016.00010.

[29] A. Delorme, S. Makeig, EEGLAB: an open source toolbox for analysis of single-trial EEG dynamics including independent component analysis, J. Neurosci. Methods 134(1) (2004) 9-21. https://doi.org/10.1016/j.jneumeth.2003.10.009.

[30] T.P. Jung, S. Makeig, C. Humphries, et al., Removing electroencephalographic artifacts by blind source separation, Psychophysiology 37(2) (2000) 163-178. https://doi.org/10.1111/1469-8986.3720163.

[31] T.W. Picton, S. Bentin, P. Berg, et al., Guidelines for using human event-related potentials to study cognition: recording standards and publication criteria, Psychophysiology 37(2) (2000) 127-152. https://doi.org/10.1111/1469-8986.3720127.

[32] M.A. Jatoi, N. Kamel, A.S. Malik, et al., EEG based brain source localization comparison of sLORETA and eLORETA, Australas. Phys. Eng. Sci. Med. 37(4) (2014) 713-721. https://doi.org/10.1007/s13246-014-0308-3.

[33] T. Hummel, A. Genow, B.N. Landis, Clinical assessment of human gustatory function using event related potentials, J. Neurol. Neurosurg. Psychiatry. 81(4) (2010) 459-464. https://doi.org/10.1136/jnnp.2009.183699.

[34] C. Destrieux, B. Fischl, A. Dale, et al., Automatic parcellation of human cortical gyri and sulci using standard anatomical nomenclature, NeuroImage 53(1) (2010) 1-15. https://doi.org/10.1016/j.neuroimage.2010.06.010.

[35] M. Sandler, A.G. Howard, M. Zhu, et al., MobileNetV2: inverted residuals and linear bottlenecks, Proc. IEEE Conf. Comput. Vis. Pattern Recognit. 2018 (2018) 4510-4520. https://doi.org/10.1109/CVPR.2018.00474.

[36] T.N. Kipf, M. Welling, Semi-supervised classification with graph convolutional networks, arXiv (2016) arXiv:1609.02907. https://doi.org/10.48550/arXiv.1609.02907.

[37] R.S. Herz, T. Engen, Odor memory: review and analysis, Psychon. Bull. Rev. 3(3) (1996) 300-313. https://doi.org/10.3758/BF03210754.

[38] C. Owen, Olfaction, emotion and memory: an investigation of the affective impact of odours in memories using the Swinburne sensory emotion association survey (SSEAS), Thesis, 2005. https://doi.org/10.25916/sut.26270356.

[39] B.E. Stein, T.R. Stanford, Multisensory integration: current issues from the perspective of the single neuron, Nat. Rev. Neurosci. 9(4) (2008) 255-266. https://doi.org/10.1038/nrn2331.

[40] M.M. Murray, M.T. Wallace, The neural bases of multisensory processes, CRC Press, 2012. https://doi.org/10.1201/9781439812174.